ELSEVIER

International Journal of Pharmaceutics 235 (2002) 247–265

international journal of pharmaceutics

www.elsevier.com/locate/ijpharm

Preparation and in vitro characterization of a eutectic based semisolid self-nanoemulsified drug delivery system (SNEDDS) of ubiquinone: mechanism and progress of emulsion formation

S. Nazzal [a], I.I. Smalyukh [b], O.D. Lavrentovich [b], Mansoor A. Khan [a,*]

[a] *Department of Pharmaceutical Sciences, School of Pharmacy, Texas Tech University Health Science Center, 1300 Coulter, Suite 400, Amarillo, TX 79106, USA*

[b] *Chemical Physics Interdisciplinary Program and Liquid Crystal Institute, Kent State University, Kent, OH 44242, USA*

Received 29 October 2001; received in revised form 20 December 2001; accepted 21 December 2001

Abstract

The objectives of the present work were, first, to develop a self-nanoemulsified drug delivery system (SNEDDS) based on the eutectic properties of ubiquinone (CoQ_{10}); and second, to study the progress of emulsion formation and drug release mechanisms by turbidimetry and droplet size analysis. Binary phase diagrams of CoQ_{10} with menthol and essential oils were constructed and used to develop the self-nanoemulsified formulation. Pseudo ternary phase diagram was constructed to identify the efficient self-emulsification region. Release mechanisms of the resultant formulas were quantified using turbidimetry in combination with dissolution studies. Turbidity time profiles revealed three distinctive regions: lag phase, plateau, and the pseudolinear phase. Lag phase was attributed to the liquid crystalline properties of the formula. Plateau turbidity was correlated with droplet size. Laser diffraction analysis revealed an average droplet diameter of 100 nm. Emulsification rate was obtained from the corrected slope of the pseudolinear phase of the profile. Stability of the formula was further evaluated using Fourier transform-infrared (FT-IR) attached to an attenuated total reflectance (ATR) accessory. The present study revealed a eutectic based semisolid self-emulsified delivery system that can overcome the drawbacks of the traditional emulsified systems such as low solubility and irreversible precipitation of the active drug in the vehicle with time.

Keywords: Coenzyme Q_{10}; Eutectic mixture; Self-nanoemulsified drug delivery system; SNEDDS; Turbidimetry; Liquid crystals

1. Introduction

Ubiquinone, also known as CoenzymeQ_{10} (CoQ_{10}) (Fig. 1), is a physiologically important compound acting as an electron shuttle in mitochondrial respiratory chain and as a stabilizing

* Corresponding author. Tel.: +1-806-356-4000x285; fax: +1-806-356-4034.
E-mail address: khan@cortex.ama.ttuhc.edu (M.A. Khan).

0378-5173/02/$ - see front matter
PII: S0378-5173(02)00003-0

agent in cellular membranes (Grossi et al., 1992). Due to its poor aqueous solubility (Kommuru et al., 1999), CoQ_{10} presented a challenge in the development of a formulation for oral administration. Many different approaches have been used to improve the in vitro dissolution of CoQ_{10}. Some of the approaches include complexation with cyclodextrins (Lutka and Pawlaczyk, 1995), solubilization in a blend of polysorbate 80 and medium chain triglycerides (Chopra et al., 1998), preparation of re-dispersable dry emulsion (Takeuchi et al., 1992), solid dispersion (Nazzal et al., 2002) and recently, development of a self-emulsified drug delivery system (Kommuru et al., 2001). Self-emulsifying drug delivery systems (SEDDS) are isotropic mixtures of oil, surfactant, co-surfactant and drug that form fine oil-in-water emulsion when introduced into aqueous phases under gentle agitation (Charman et al., 1992; Craig et al., 1993).

In the traditional methods of preparing self-emulsified delivery systems, active ingredients are dissolved in fixed oils or triglycerides and subsequently blended with suitable solubilizing agents. However, due to limited solubility of some drugs in these oils, such methods often result in low drug loading (Kang et al., 2000) and suffer from irreversible precipitation of the active ingredient and/or the excipient with time (Kommuru et al., 2001). It was therefore of interest to determine whether reversibly induced re-crystallized semisolid self-nanoemulsifying drug delivery systems (SNEDDS) could be considered as an eventual alternative to the conventional self-emulsifying vehicles. Such systems could be prepared from a eutectic interaction between the drug and a suitable carrying agent. In eutectic based self-nanoemulsified systems, the melting point depression method allows the oil phase containing the drug itself to melt at body temperature from its semisolid consistency and disperse to form emulsion droplets in nanometer size range. Emulsion systems based on a eutectic mixture of lidocaine–prilocaine (Nyqvist-Mayer et al., 1986), and lidocaine–menthol (Kang et al., 2000) were used in the preparation of topical formulations. However, little is known about the use of eutectic mixtures for the preparation of self-emulsified formulations.

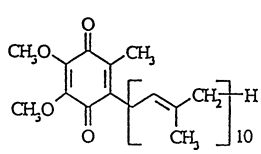

Fig. 1. Structure of CoQ_{10}.

In recent years there was a growing interest in the lipid based formulations as a method for delivering poorly soluble drugs. Pseudoternary phase diagrams are often used to visually describe the spontaneity of emulsion formation. However, little has been done to quantify the release patterns of these emulsions from their dosage forms and to identify the liquid crystals associated with the progress of emulsion formation during the early stages of the disruption process.

The objectives of the present study were, first, to develop a SNEDDS based on the eutectic properties of ubiquinone (CoQ_{10}), and second, to study the progress of emulsion formation and drug release mechanisms by turbidimetry and droplet size analysis.

2. Materials and methods

2.1. Materials

CoQ_{10} was a generous gift from Kyowa Hakko, USA (New York, NY). Polyoxyl 35 castor oil (cremophor EL) was obtained from BASF Corp. (Mount Olive, NJ). Medium chain mono- and diglycerides (capmul MCM-C8) was obtained from Abitec Corp. (Janesville, WI). L-menthol, anise oil, peppermint oil and spearmint oil were purchased from Spectrum Inc. (Gardena, CA). Single fold lemon oil was purchased from Young Living (Payson, UT). Hydroxypropyl methylcellulose (HPMC) capsules were supplied by Shionogi Qualicaps (Whitsett, NC). HPLC grade methanol and *n*-hexane were purchased from VWR Scientific (Minneapolis, MN). All the chemicals were used as received.

2.2. Methods

2.2.1. Differential scanning calorimetry (DSC) of CoQ_{10}-menthol and CoQ_{10}-essential oil binary systems.

CoQ_{10} and L-menthol were mixed at various ratios between 90:10 and 10:90 (w/w). Approximately 5 mg of the mixture was sealed in the aluminum pan and analyzed using a differential scanning calorimeter (DSC 7, Perkin–Elmer, Norwalk, CT). Thermal analysis was carried out between 25 and 60 °C under nitrogen gas flow against an empty reference pan at a heating rate of 10 °C min^{-1}. Similarly, different ratios of CoQ_{10} and the essential oil between 80:20 and 20:80 (w/w) were mixed and melted at 37 °C. Resulting oils were stored at 4 °C for 24 h to allow complete re-crystallization of CoQ_{10}. To avoid oil evaporation, approximately 10 mg of the mixture was weight onto a DSC sample pan and kept in an airtight container during storage prior to DSC analysis. For CoQ_{10}-essential oil mixtures at ratios between 80:20 and 60–40 (w/w), thermal analysis was carried out between 25 and 55 °C. Samples with higher essential oil concentration were analyzed between 10 and 40 °C. Heating rate used was 10 °C min^{-1}. Lower temperatures were maintained using refrigerated cooling accessory (Intracooler 2, Perkin–Elmer).

2.2.2. Determination of CoQ_{10} melting time

CoQ_{10} was accurately weighed and mixed with 50 and 60% w/w of peppermint oil, spearmint oil, anise oil or lemon oil in a screw-capped glass vials. Mixtures were allowed to melt at 37 °C in water bath (Ikamag® Ret-G, Terochem Scientific, Toronto, Canada). Cremophor EL was added to the melt at a concentration of 20, 40 and 60% w/w of the final weight using a positive displacement pipette (Microman®, Gilson Inc., Middleton, WI) and stirred with a magnetic bar. Vials were then capped and stored at ambient temperatures in tight containers protected from light. After 24 h sample vials containing the solidified preparations were immersed in water bath maintained at 37 °C. Samples were monitored for a change in their physical appearance and the time was recorded until a complete melt was obtained.

2.2.3. Formulation of the self-emulsified systems

A series of self-emulsifying systems were prepared with varying concentrations of the oily mix (37.5–60%), cremophor EL (0–62.5%), and capmul MCM-C8 (0–62.5%). The oily mix consisted of CoQ_{10} and lemon oil at a ratio of 50:50. CoQ_{10} and lemon oil were accurately weighed into screw-capped glass vial and melted in a water bath at 37 °C. Cremophor EL and capmul MCM-C8 were added to the oily mix using a positive displacement pipette and stirred with a magnetic bar. While molten, formulations with different concentrations of surfactant, co-surfactant, and the oil mix, each containing CoQ_{10} at a final loading of 30 mg, were filled into size 4 HPMC capsules. Filled capsules were stored at room temperature until their use in subsequent studies.

2.2.4. Visual observations

To assess the self-emulsification properties, formulation (50 mg) pre-melted at 37 °C was introduced into 100 ml of water in a glass Erlenmeyer flask at 25 °C and the contents were gently stirred manually. The tendency to spontaneously form a transparent emulsion was judged as 'good', and it was judged 'bad' when there was poor or no emulsion formation (Craig et al., 1995; Kommuru et al., 2001). Phase diagrams were constructed identifying the good self-emulsifying region. All studies were repeated in triplicates with similar observations being made between repeats.

2.2.5. Emulsion droplet size analysis and turbidity measurements

Formulation (50 mg) melted at 37 °C was diluted with water, pre-equilibrated at 37 °C, to 100 ml in an Erlenmeyer flask and gently mixed with hand. The resultant emulsions was evaluated for its droplet size and turbidity as follow.

2.2.5.1. Droplet size analysis. The droplet size distribution of the resultant emulsions was determined by laser diffraction analysis using Coulter particle size analyzer (Model LS230, Miami, FL), which has a particle size measurement range of 0.04–2000 μm. The sizing of the emulsions was determined in a small volume module. Samples were directly placed into the module and the data

were collected for 60 s. Particle size was calculated from the volume size distribution. All studies were repeated, with good agreement being found between measurements.

2.2.5.2. Turbidity measurement. Turbidity of the resultant emulsions given in nephlometric turbidity units (NTU) was measured using HACH turbidimeter (Model 2100AN, Loveland, CO). Turbidity measurements were performed on 30 ml of the emulsion stored in a clear screw-capped sample vials. HACH 2100AN turbidimeter used in the study was carefully calibrated with formazin standards. Accuracy at the lower range of turbidity is essential especially for small and diluted emulsions with high surfactant concentrations. The largest source of error at low turbidities is the stray light, that is, the light that reaches the detector due to sources other than sample turbidity (Sadar, 1998). Accuracy of the HACH 2100 AN turbidimeter, as specified by the manufacturer and based on instrument calibration, is approximately ± 0.01 NTU with stray light less than or equal to 0.01 NTU.

2.2.6. Fourier transform-infrared spectroscopy (FT-IR)

FT-IR spectroscopy was performed using FTIR model Nicolet Impact 410 (Thermo Nicolet, Madison, WI) attached to an attenuated total reflectance (ATR) accessory (DuraSampI/R, SensIR Technologies, Danbury, CT). ATR was fitted with a single bounce diamond at 45° internally reflected incident light providing a sampling area of 1 mm in diameter with a sampling depth of several microns. Samples analyzed were CoQ_{10} powder, a 50:50 CoQ_{10}–lemon oil melt, a solidified 50:50 CoQ_{10}–lemon oil mix and a solidified mixture of lemon oil, CoQ_{10}, cremophor EL and capmul MCM-C8 at a ratio of 0.5:0.5:1:1. Samples were prepared as described above. A small amount of the sample was directly placed on the diamond disk and scanned for absorbance over the range from 4000 to 500 wavenumbers (cm^{-1}) at a resolution of 1 cm^{-1}.

2.2.7. Dissolution studies

Dissolution profiles of the capsules filled with the self-nanoemulsified formulations were determined using USP XXIII rotating paddle apparatus (VanKel, mod. VK7000, Cary, NC) at 37 °C and a rotating speed of 50 rpm in a 900 ml of water. Capsules were held to the bottom of the vessel using copper sinkers. Samples (3 ml) withdrawn after 15 min were filtered using a 10 μm VanKel filter and assayed for CoQ_{10} by the HPLC method reported in the HPLC analysis section. The dissolution experiments were carried out in triplicates.

2.2.8. Turbidimetry

Turbidity profiles of the capsules filled with the self-emulsified formulations were determined using HACH turbidimeter (Model 2100AN). Low-pressure flow cell was used to allow directly reading sample turbidity associated with capsules subjected to the same dissolution conditions as described above. Two 1/8 in. tygon tubings were connected to the pump attached to the dissolution autosampler (VanKel, mod. VK8000). First tubing was installed between the pump and the inlet of the flow cell while the other connected the pump to the dissolution vessel. Inlet of the tube connecting the pump to the dissolution vessel was covered with a 40 μm nylon screen and immersed into the medium so that the sample can be continuously withdrawn from a zone midway between the surface of the medium and the top of the rotating blade. Another tubing was installed to the outlet of the flow cell leading back to the dissolution vessel. Before the start of the experiments, deionized water was pumped through the flow cell until a reading below 0.150 NTU was maintained. Throughout the study, dissolution medium was continuously pumped into the flow cell and back to the dissolution vessel. The turbidimeter was set so that a reading was recorded on the attached printer every 15 s. Turbidimetry experiments were carried out in triplicates.

2.2.9. Optical polarizing microscopy studies

To verify the liquid crystalline properties of the mixtures of surfactant (cremophor EL), co-surfactant (capmul MCM-C8) and water, optical bire-

fringence of the mixtures was examined under a microscope with crossed polarizers (Nikon Eclipse E600 Pol, Nikon Instech Co., Japan) equipped with a CCD camera (Hitachi HV-C20, Hitachi America, Ltd., San Diego, CA). The mixtures were prepared by first mixing the co-surfactant and water and then adding the surfactant. The compositions in glass tubes were mixed acoustically and then placed into a centrifuge (Centra MP4R, International Equipment Company, Needham Heights, MA) for 0.5–1 h at 3000 rpm (RCF equivalent to $500 \times g$). Ultrapure water with specific resistance of better than or equal to 16 MΩ cm and pH around 4 was used. The test samples for polarizing microscopy studies were prepared in rectangular glass capillaries (gap thickness 100 μm and width 1 mm, length 5 cm). Both ends were sealed with epoxy resin.

2.2.10. HPLC Analysis

Detailed HPLC method for the analysis of aqueous CoQ_{10} samples was described by Nazzal et al. (2001). Briefly, CoQ_{10} was analyzed at ambient temperature utilizing a C18, 3.9×150 mm reverse phase chromatography column (Nova-Pak; Waters, Milford, MA). The mobile phase consisted of methanol:*n*-hexane (9:1) and was pumped at a flow rate of 1.5 ml min^{-1}. The Waters HPLC instrument consisted of a 510 pump, 712 WISP autosampler, and a 490E UV detector set at a wavelength of 275 nm. The chromatographic data was managed using STAR 5.3 software (Varian, Walnut Creek, CA).

3. Results and discussion

3.1. DSC studies of the binary CoQ_{10}–menthol and CoQ_{10}–essential oil systems

CoQ_{10} was found to form an eutectic mixture with L-menthol. DSC thermograms of the binary system of CoQ_{10} with menthol at different ratios are given in Fig. 2. The major endotherms at 51.7 and 44.1 °C represent the melting point of CoQ_{10} and L-menthol, respectively. Based on the thermal analysis data a binary phase diagram was constructed and is given in Fig. 3. As seen from the figure the eutectic melting point lies between 30 and 60% w/w CoQ_{10}. Within the binary system, depression in melting temperature of CoQ_{10}, however, was limited to temperatures exceeding 37 °C. Thus, an oily melt can not be obtained at or below body temperature. A gradual shift and reformation of the original CoQ_{10} endothermic peak was observed when the samples within the binary system were left uncovered and analyzed after 1 week. The volatile ingredients of menthol are responsible for the physical changes in CoQ_{10}, i.e. depression in its melting temperature. To validate this observation, the effect of peppermint oil as a representative volatile ingredient of menthol crystals and three additional volatile oils namely, spearmint oil, lemon oil and anise oil were investigated for their effect on the melting thermograms of CoQ_{10}. Thermal analysis and the DSC data of the binary system of CoQ_{10} with peppermint oil are given in Fig. 4. A binary phase diagram of CoQ_{10} with the essential oils was constructed and is given in Fig. 5. Thermograms of the mixtures clearly indicated that these compounds formed binary eutectic systems. An increase in percent essential oil causes a gradual decrease in the melting temperature of CoQ_{10}. At sufficient concentration of the volatile oil it becomes feasible to convert CoQ_{10} into an oily phase at or below body temperatures.

3.2. Determination of CoQ_{10} melting times

Due to the limited solubility of CoQ_{10} in fixed oils and triglycerides (Kommuru et al., 2001), the melting point depression method using essential oils provides an attractive alternative for the preparation of an emulsified formulation. A number of essential oils are used for their flavors and odors and are recognized by the Code of Federal Regulations as GRAS (generally recognized as safe) compositions that do not require regulatory agency approval before they are included in ingested material (CFR, Title 21, parts 182.10, 182.20, 182.40, 182.50, 182.60, 172.510, and 172.515). Essential oils have shown to increase the oral bioavailability of cyclosporine by inhibiting *P*-glycoprotein efflux transporter and by decreasing drug biotransformation in the gut wall by

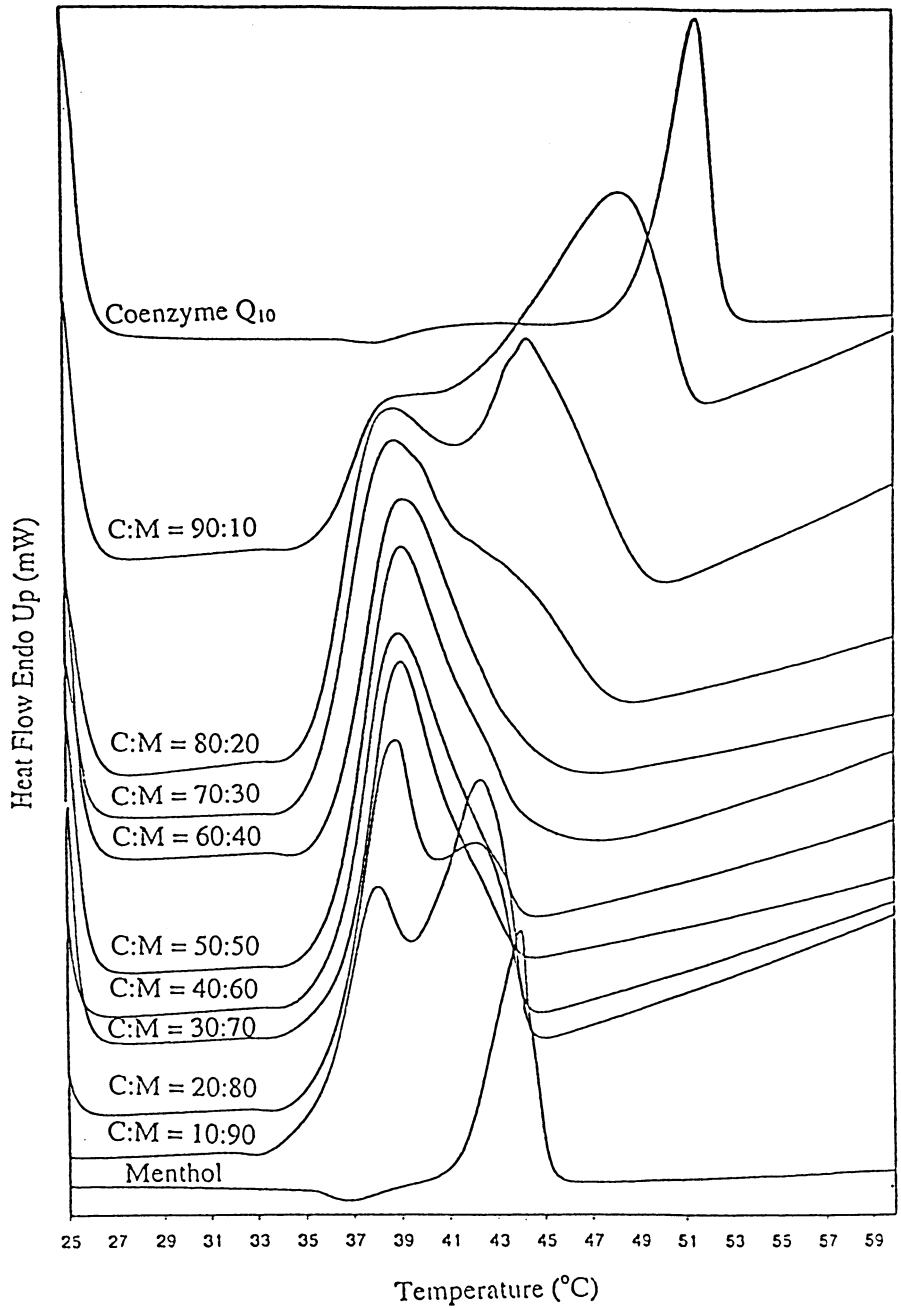

Fig. 2. DSC thermograms of CoQ_{10}, L-menthol, and their binary mixtures. Ratios by weight.

inhibiting cytochrome P450 (Benet et al., 1998). A preparation could be made at which body temperature is used to melt a system comprising essential oil, CoQ_{10} and an emulsifier when the essential oil is added in an amount sufficient to lower the melting temperature of CoQ_{10} to or below 37 °C. Essential oils, however, should be effective as eutectic agents in the presence of other liquid

excipients. Table 1 demonstrates the feasibility of the described approach. Four essential oils, spearmint oil, peppermint oil, lemon oil, and anise oil, were evaluated for their eutectic efficacy in the presence of other formulation excipients. Due to limited solubility of CoQ_{10} in surfactants (Kommuru et al., 2001) the use of cremophor EL as a model emulsifier not only induces crystallization of CoQ_{10} in the cooled supersaturated mixture but also may delay or retard re-melting the system at higher temperatures. The time necessary to melt different combinations of CoQ_{10}, essential oil and cremophor EL at 37 °C was recorded. When 60% w/w of cremophor EL was added, preparations made with 50 and 60% w/w lemon oil to CoQ_{10} melted within 5.3 and 1.8 min, respectively. Precipitation of CoQ_{10} at higher cremophor EL concentration for the formulas made with anise oil, peppermint oil and spearmint oils was however irreversible rendering them less effective for the preparation of emulsified systems. The use of lemon oil appears reasonable and attractive. At 50% w/w of lemon oil to CoQ_{10}, formulas would melt within 5 min from initial exposure to body temperatures. In this case, recrystallization of CoQ_{10} becomes advantageous in the production of a stable semisolid product compared with the existing liquid formulas with the potential of irreversible precipitation and separation of the active ingredient due to supersaturation or fluctuation in storage temperatures (Kommuru et al., 2001). Furthermore, lemon oil has been used internally as herbal medicine for acidic disorders such as arthritis and rheumatism with great benefit in liver congestion (Lawless, 1995).

3.3. Visual observations

For the development of a self-emulsified formulation, a right blend of low and high HLB surfactants is necessary for the formation of a stable microemulsion (Craig et al., 1995; Pouton, 2000). Therefore, a high HLB surfactant (cremphor EL) and a low HLB co-surfactant (capmul MCM-C8) were selected. A ratio of 50:50 of lemon oil to CoQ_{10} was selected as the oil phase. Spontaneity of the formula was evaluated as described in the experimental section. The pseudo ternary phase diagram of the system comprising the surfactant, co-surfactant and the oily phase was constructed and is given in Fig. 6. Area enclosed within the solid line represents the region of self-emulsifica-

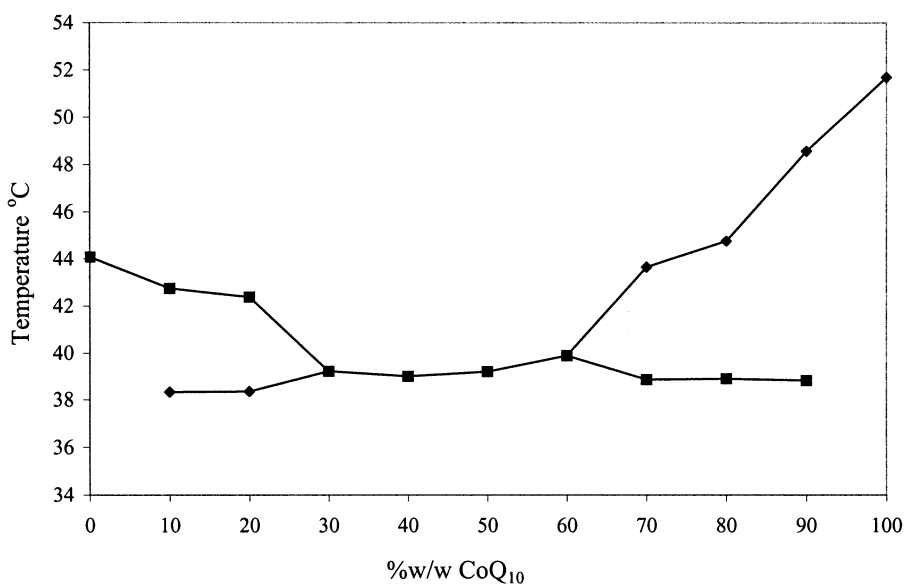

Fig. 3. The temperature/composition phase diagram of CoQ_{10}–menthol binary system determined by DSC.

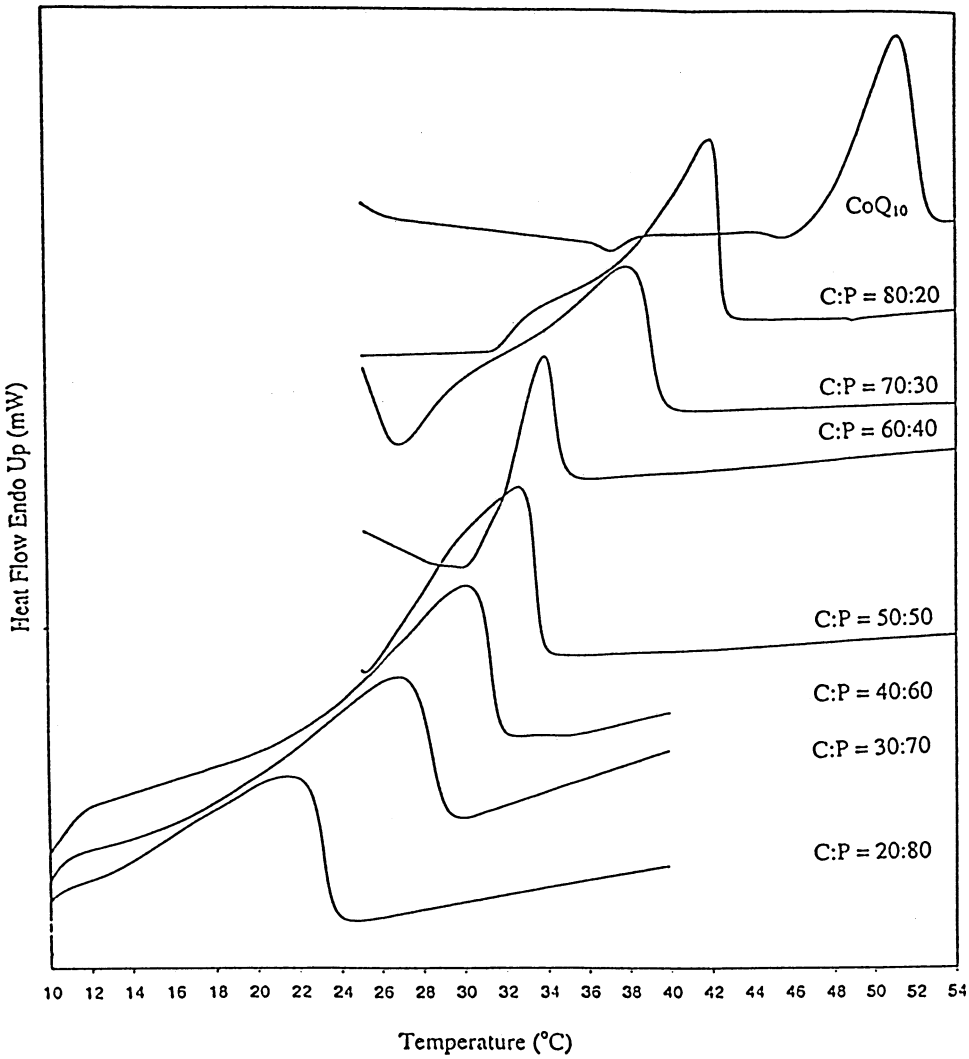

Fig. 4. DSC thermograms of CoQ_{10}, peppermint oil, and their binary mixtures. Ratios by weight.

tion. Within this area a ternary mixture forms a fine oil in water emulsion with only gentle agitation. This is possible as surfactants strongly localized to the surface of the emulsion droplet reduces interfacial free energy and provide a mechanical barrier to coalescence resulting in a thermodynamically spontaneous dispersion (Reiss, 1975). Furthermore, co-surfactants increase interfacial fluidity by penetrating into the surfactant film creating void space among surfactant molecules (Constantinides and Scalart, 1997). Constraints on the formulas were placed so that oil phase was not less than 37.5% to ensure melting of the crystallized product based on the early predictions given in Table 1, and did not exceed 63% to ensure efficient CoQ_{10} emulsification.

3.4. Droplet size analysis and turbidity measurements

Droplet size distribution of the systems within the area of self-emulsification is given in Table 2.

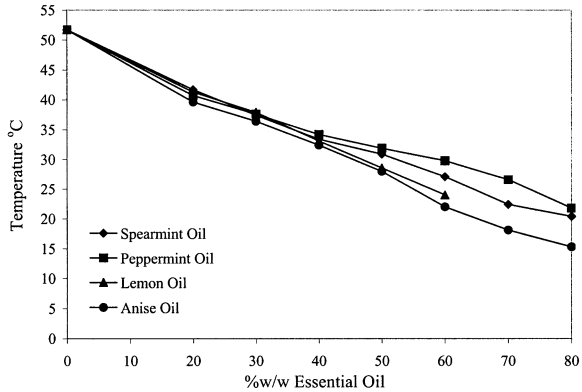

Fig. 5. The temperature/composition phase diagram of CoQ_{10}–essential oil binary systems determined by DSC.

The effect of surfactant to co-surfactant ratio on droplet size is given in Fig. 7. At ratios greater than 0.5, globule size was relatively constant at about 100 nm and independent on any component of the ternary system. It was only at ratios smaller than 0.5 when globule size increased and became greatly dependent on cremophor EL and capmul MCM-C8 concentrations yet independent

Table 1
Melting time for the given mixtures of CoQ_{10}, essential oil and cremophor EL at 37 °C

CrEL (%)[b]	20%	40%	60%
Spearmint Oil[a]			
60%	0.69 ± 0.13[c]	1.56 ± 0.59	N/A
50%	4.38 ± 2.13	N/A[d]	N/A
Peppermint Oil			
60%	1.11 ± 0.42	N/A	N/A
50%	8.17 ± 2.08	N/A	N/A
Anise Oil			
60%	0.83 ± 0.73	0.97 ± 0.27	N/A
50%	1.28 ± 0.63	2.33 ± 0.88	N/A
Lemon Oil			
60%	1 ± 0.17	1.29 ± 0.44	1.76 ± 0.23
50%	2 ± 0.29	3.56 ± 1.69	5.33 ± 1.48

[a] Percent w/w of essential oil in the binary mixture of the essential oil with CoQ_{10}.

[b] Percent w/w of cremophor EL in the final mixture of CoQ_{10}, essential oil and cremophor EL.

[c] Time is given in minutes.

[d] Not applicable. No melting was observed within 24 h.

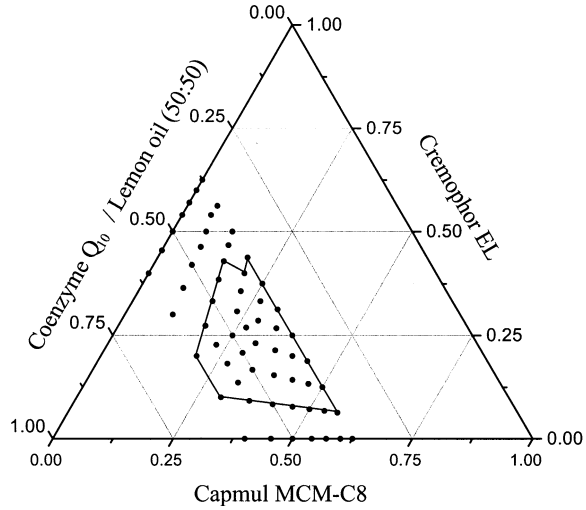

Fig. 6. Pseudo-ternary phase diagram indicating the efficient self-emulsification region (key, the region of efficient self-emulsification is bound by the solid line; and the filled circles represent the compositions which were evaluated).

on the added oil phase. Gao et al. (1998) have reported similar observations with the microemulsion containing captex-355, cremophor EL, transcutol and saline where the droplet size decreased with increasing surfactant to co-surfactant ratio and became constant at a ratio above 2:1. It was reported that the addition of surfactants to the microemulsion systems causes the interfacial film to stabilize and condense, while the addition of co-surfactant causes the film to expand (Constantinides and Scalart, 1997; Gao et al., 1998). Comparison of droplet size data with the visual observations shows that good emulsification properties are reflected by the low globule size with the exception of the formula made with high capmul MCM-C8 to cremophor EL ratios. This reflects the fact that the visual test is a measure of the spontaneity of emulsification rather than a measure of the quality of the formed emulsion (Craig et al., 1995). Turbidity, given in NTU, was measured for the same samples utilized for particle size analysis. Turbidity readings ($NTU_{observed}$) are given in Table 3.

In theory, a beam of light passing through a cloud of small particles will be scattered by the particles in all directions. Measuring the light

Table 2
Effect of SNEDDS composition on the emulsion droplet size distribution

Formulations	SNEDDS composition (% w/w)					SNEDDS emulsion droplet size (μm)					
	CoQ10	Lemon oil	Capmul	Cremophor	Mean	Span	$D(0.1)$	$D(0.25)$	$D(0.5)$	$D(0.75)$	$D(0.9)$
1	18.8	18.8	56.3	6.3	2.817	0.270	3.179	3.014	2.806	2.619	2.468
2	18.8	18.8	50.0	12.5	0.402	0.277	0.845	0.572	0.323	0.117	0.110
3	18.8	18.8	43.8	18.8	0.121	0.015	0.142	0.130	0.119	0.100	0.101
4	18.8	18.8	37.5	25.0	0.112	0.037	0.165	0.135	0.106	0.084	0.070
5	18.8	18.8	31.3	31.3	0.090	0.012	0.107	0.099	0.089	0.081	0.045
6	18.8	18.8	25.0	37.5	0.113	0.017	0.137	0.125	0.112	0.100	0.092
7	18.8	18.8	18.8	43.8	<0.040						
8	20.0	20.0	53.3	6.7	0.845	0.308	1.287	1.027	0.786	0.607	0.499
9	20.0	20.0	46.7	13.3	0.725	0.213	1.031	0.862	0.693	0.558	0.472
10	20.0	20.0	40.0	20.0	0.121	0.048	0.170	0.141	0.110	0.083	0.067
11	20.0	20.0	33.3	26.7	0.089	0.026	0.107	0.098	0.089	0.081	0.074
12	20.0	20.0	26.7	33.3							
13	20.0	20.0	20.0	40.0	0.105	0.025	0.117	0.107	0.099	0.091	0.084
14	21.4	21.4	50.0	7.1	0.691	0.201	0.967	0.811	0.657	0.538	0.461
15	21.4	21.4	42.9	14.3	0.219	0.148	0.427	0.278	0.173	0.112	0.082
16	21.4	21.4	35.7	21.4	0.116	0.015	0.136	0.126	0.115	0.105	0.097
17	21.4	21.4	28.6	28.6							
18	21.4	21.4	21.4	35.7	0.110	0.029	0.122	0.115	0.105	0.096	0.087
19	21.4	21.4	14.3	42.9	0.088	0.025	0.098	0.089	0.079	0.072	0.067
20	23.1	23.1	46.2	7.7	0.757	0.422	1.338	1.015	0.713	0.464	0.187
21	23.1	23.1	38.5	15.4							
22	23.1	23.1	30.8	23.1	0.122	0.021	0.151	0.136	0.120	0.106	0.096
23	23.1	23.1	26.9	26.9	0.115	0.027	0.128	0.122	0.110	0.102	0.091
24	23.1	23.1	23.1	30.8	0.106	0.029	0.115	0.110	0.107	0.096	0.089
25	23.1	23.1	15.4	38.5	0.103	0.027	0.128	0.107	0.098	0.089	0.081
26	25.0	25.0	41.7	8.3	0.575	0.114	0.735	0.652	0.564	0.486	0.430
27	25.0	25.0	33.3	16.7	0.119	0.026	0.155	0.136	0.116	0.099	0.087
28	25.0	25.0	29.2	20.8	0.122	0.021	0.151	0.136	0.120	0.106	0.096
29	25.0	25.0	25.0	25.0	0.120	0.015	0.140	0.131	0.120	0.109	0.103
30	25.0	25.0	16.7	33.3	0.092	0.024	0.107	0.095	0.086	0.081	0.073
31	27.3	27.3	36.4	9.1	0.679	0.338	0.829	0.688	0.520	0.393	0.297
32	27.3	27.3	31.8	13.6	0.126	0.016	0.147	0.136	0.125	0.114	0.105
33	27.3	27.3	27.3	18.2	0.124	0.006	0.132	0.129	0.124	0.118	0.114
34	27.3	27.3	22.7	22.7	0.113	0.015	0.133	0.123	0.113	0.103	0.095
35	27.3	27.3	18.2	27.3	0.119	0.014	0.141	0.130	0.119	0.109	0.102
36	30.0	30.0	30.0	10.0	0.321	0.037	0.371	0.345	0.319	0.294	0.274
37	30.0	30.0	20.0	20.0	0.124	0.016	0.145	0.134	0.123	0.112	0.104

received at an angle normal to the concentric light beam provides indications on size and number of scattered particles (Groves and Mustafa, 1974). Light scattering by colloids conforms to Rayleigh theory, which predicts that light scattering or measured turbidity τ in a simplified equation can be given by

$$\tau = Knv^2$$

where K is a machine constant, v the particle volume and n is the number of particles (Groves and Mustafa, 1974; Pouton, 1985).

The effect of surfactant to co-surfactant ratio of the emulsified formulas on $NTU_{obsreved}$ and $NTU_{plateau}$ turbidity readings is given in Fig. 7. As seen in the plot, turbidity follows the same trend as droplet size. Pouton (1985) has reported a linear correlation between the intensity of the scattered light and the squared volume of the dispersed droplets. Hence, NTU could be directly used to predict relative droplet size of the emulsion. To give a sense about the clarity of the formulas, turbidity of drinking water ranges from 0 to 1 NTU (Hongve and Akesson, 1998).

3.5. Fourier transform-infrared spectroscopy (FT-IR)

The ease of handling aqueous solutions and semisolid preparations is one of the major advantages of ATR used in conjugation with FT-IR spectrometry (Yang and Her, 1999). CoQ_{10} compatibility with the excipients of self-nanoemulsified preparation can be tested with FT-IR. Absorbance spectrums of CoQ_{10} and lemon oil are given in Fig. 8. CoQ_{10} spectrum showed several (29) sharp characteristic peaks. The spectrum of the 50:50 melt of CoQ_{10} and lemon oil, given in Fig. 8, had features of each of the components with the expected peak broadening due to its amorphous character whereas a sample of the solidified mixture had sharp lines and resembled the CoQ_{10} spectrum in every detail. Lemon oil did not change the infrared spectrum of CoQ_{10} indi-

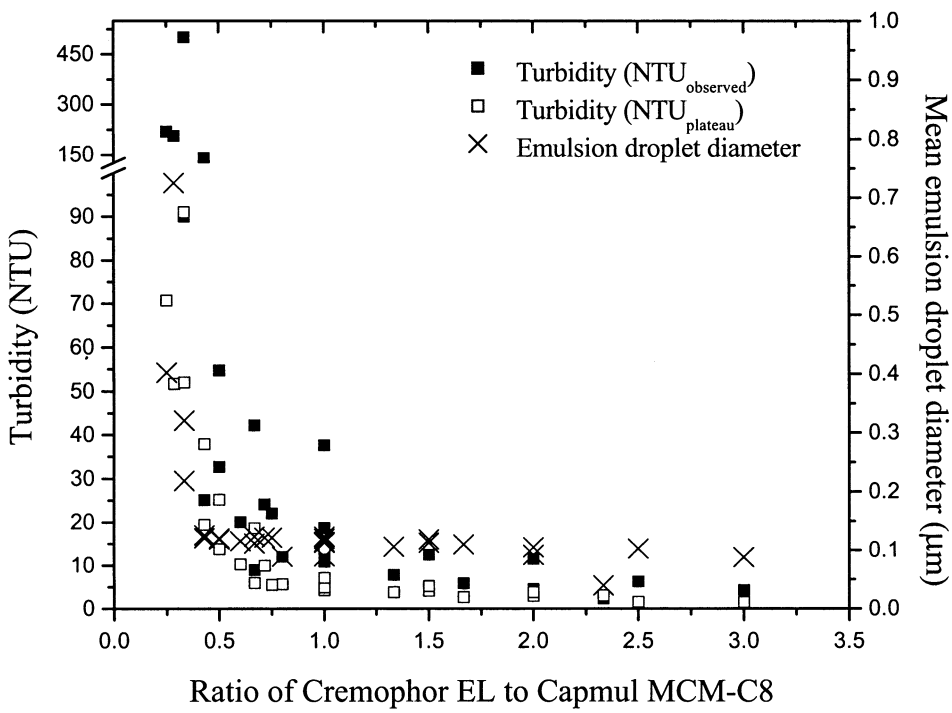

Fig. 7. Effect of surfactant (cremophor EL) to co-surfactant (capmul MCM-C8) ratios on mean droplet size diameter, and on $NTU_{observed}$ and $NTU_{plateau}$ turbidity values.

Table 3
Effect of SNEDDS composition on turbidity readings and the cumulative amount of CoQ10 released after 15 min

Formulations	SNEDDS composition (% w/w)				SNEDDS turbidity			CoQ10 released (15 min)	
	CoQ10	Lemon oil	Capmul	Cremophor	NTUobsrved	NTUexp	NTUplateau	Percent released	STD
1	18.8	18.8	56.3	6.3	605.5				
2	18.8	18.8	50.0	12.5	220.0	78.2	70.7	94.0	2.18
3	18.8	18.8	43.8	18.8	25.1	8.9	19.5	90.3	7.87
4	18.8	18.8	37.5	25.0	9.0	3.2	6.0	92.8	2.52
5	18.8	18.8	31.3	31.3	6.9	2.5	4.8	88.8	2.52
6	18.8	18.8	25.0	37.5	5.3	1.9	4.1	88.0	2.84
7	18.8	18.8	18.8	43.8	2.4	0.8	3.1	87.4	4.42
8	20.0	20.0	53.3	6.7	513.0				
9	20.0	20.0	46.7	13.3	207.0	69.0	51.7	85.0	1.14
10	20.0	20.0	40.0	20.0	32.7	10.9	13.8	87.3	1.14
11	20.0	20.0	33.3	26.7	12.0	4.0	5.7	91.0	5.35
12	20.0	20.0	26.7	33.3	7.0	2.3	3.5	96.3	1.28
13	20.0	20.0	20.0	40.0	4.5	1.5	3.0	99.5	0.64
14	21.4	21.4	50.0	7.1	510.5				
15	21.4	21.4	42.9	14.3	90.1	28.0	52.0	89.8	3.98
16	21.4	21.4	35.7	21.4	20.1	6.2	10.3	94.7	0.05
17	21.4	21.4	28.6	28.6	10.6	3.3	4.1	94.7	1.12
18	21.4	21.4	21.4	35.7	5.9	1.8	2.7	90.6	0.85
19	21.4	21.4	14.3	42.9	4.3	1.3	1.5	95.2	0.46
20	23.1	23.1	46.2	7.7	523.0				
21	23.1	23.1	38.5	15.4	90.2	26.0	34.6	93.1	0.26
22	23.1	23.1	30.8	23.1	22.1	6.4	5.5	92.6	0.28
23	23.1	23.1	26.9	26.9	10.9	3.1	4.3	86.7	0.61
24	23.1	23.1	23.1	30.8	7.8	2.3	3.8	87.9	1.61
25	23.1	23.1	15.4	38.5	6.3	1.8	1.6	89.5	0.01
26	25.0	25.0	41.7	8.3	440.0				
27	25.0	25.0	33.3	16.7	54.8	14.6	25.2	89.2	7.41
28	25.0	25.0	29.2	20.8	24.1	6.4	10.0	96.4	2.28
29	25.0	25.0	25.0	25.0	13.2	3.5	5.0	99.4	3.03
30	25.0	25.0	16.7	33.3	11.5	3.1	3.8	98.9	2.03
31	27.3	27.3	36.4	9.1	594.5				
32	27.3	27.3	31.8	13.6	141.5	34.6	37.9	92.3	0.50
33	27.3	27.3	27.3	18.2	42.2	10.3	18.7	100.1	0.35
34	27.3	27.3	22.7	22.7	18.8	4.6	7.1	98.7	0.35
35	27.3	27.3	18.2	27.3	12.5	3.1	5.2	97.8	0.17
36	30.0	30.0	30.0	10.0	501.0	111.3	91.1	98.1	1.50
37	30.0	30.0	20.0	20.0	37.6	8.3	13.9	98.2	0.33

cating no chemical interaction in the binary system and that the molecular structure of CoQ_{10} remained completely intact. Similarly, when cremophor EL and capmul MCM-C8 were added to the CoQ_{10}–lemon oil mix and the solidified mixture was analyzed, the resulting spectrum given in the figure had the characteristic CoQ_{10} bands at 1608 and 1643 cm^{-1} corresponding to the benzoquinone ring and the mono substituted isoprenoid units, respectively. The results obtained indicate that CoQ_{10} reforms to its original crystalline state when the formulation is allowed to solidify.

3.6. Dissolution and emulsification studies

To assess spontaneity and efficacy of emulsification, the methods reported by Pouton (1985), Groves and Mustafa (1974) were modified and adapted in the present study. Turbidity of the dispersion and the relative intensity of the scattered light was correlated with time during the emulsification process. Unlike the approach of Pouton (1985) current design confines to the standard compendial requirements for conducting dissolution experiments. Utilizing the flow through attachment, turbidity was directly measured using standard dissolution apparatus at 37 °C and controlled paddle rotating speed. Prepared formulations were filled into HPMC capsules. HPMC

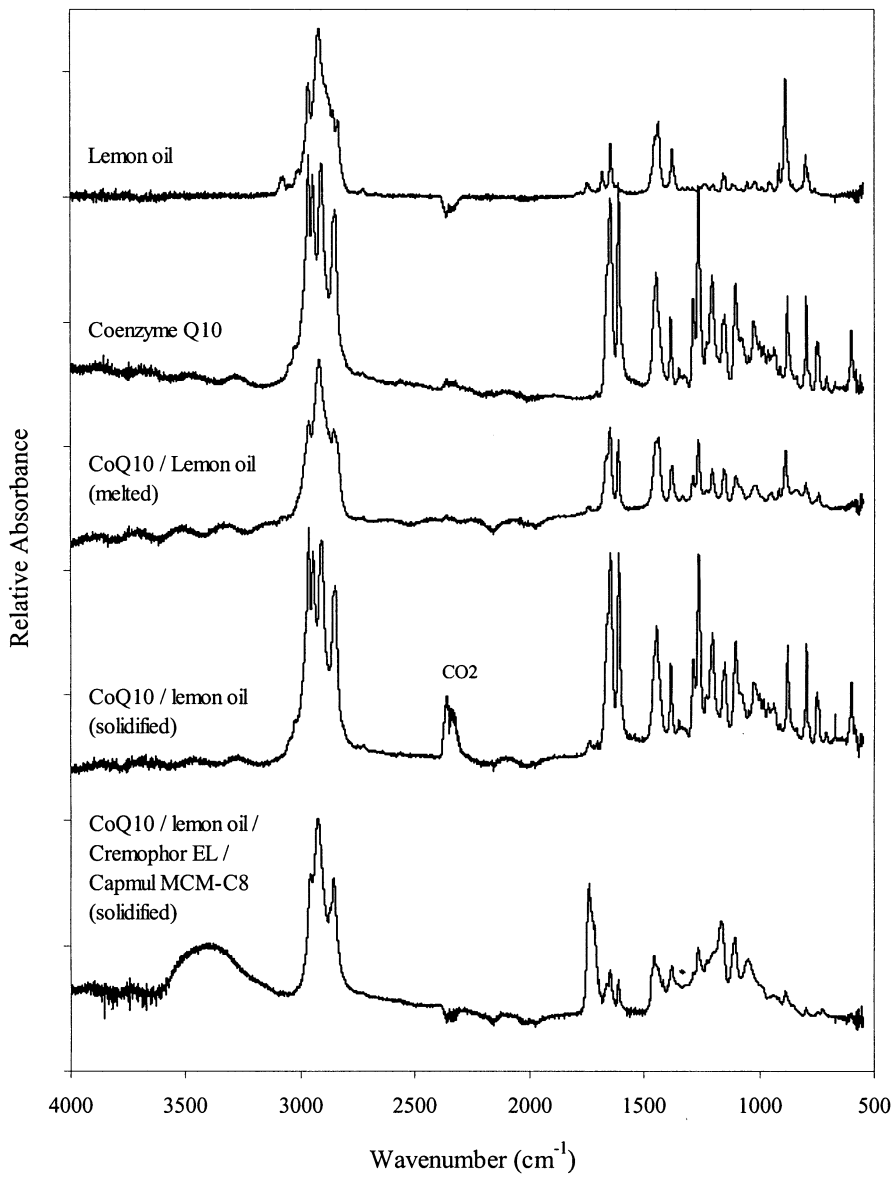

Fig. 8. FT-IR spectra of CoQ_{10} and lemon oil, and the effect of re-crystallization on the IR spectra of different CoQ_{10} mixtures.

capsules have shown to dissolve at longer times compared with standard gelatin capsules (Chiwele et al., 2000). Average dissolution time for an HPMC capsule size 4, 3 and 0 in water at 37 °C was 300, 250 and 120 s, respectively. These values are in agreement with the reported data (Chiwele et al., 2000) correlating dissolution times with the size of an HPMC capsule. Extra time provided by HPMC capsules allows the formula to completely melt at body temperature before its exposure to body fluids. Representative dissolution curves monitored by turbidimetry for three formulations, formulations 19, 32 and 36 (Tables 2 and 3) are given in Fig. 9a. Due to large number of readings obtained, plots of turbidity against emulsification time have the characteristic lag phase, pseudo linear phase and a gradual tailing toward a plateau as the emulsion systems approached equilibrium (Pouton, 1985). Similar profiles were obtained for all the formulations reported in Tables 2 and 3. Actual cumulative amount of CoQ_{10} released after 15 min for the preparations was measured by HPLC and is given in Table 3. CoQ_{10} was completely released and dispersed form all formulations into the medium within 15 min.

NTU values obtained for the solidified samples placed in the dissolution medium at 37 °C after reaching an equilibrium could be termed $NTU_{plateau}$. In order to demonstrate the efficacy of emulsion formation before and after solidification $NTU_{observed}$, which were previously determined for the melted samples while measuring droplet size, could be roughly correlated with $NTU_{plateau}$. However, since the concentration of the formulas used in both experiments were different, $NTU_{observed}$ could be corrected by a dilution factor in order to obtain the predicted NTU readings ($NTU_{expected}$). $NTU_{expected}$ are the expected plateau NTU when melted samples are introduced to a 900 ml of the dissolution medium. Since turbidity is a linear function (Jonker, 1952; Pouton, 1985) $NTU_{expected}$ could be directly predicted from $NTU_{observed}$ by applying:

$$NTU_{expected} = \frac{C_2 \times NTU_{observed}}{C_1}$$

where C_2 is the concentration of the formula used in the dissolution study i.e. formula weight/900 ml of the dissolution medium and C_1 is the concentration of the formula used for measuring $NTU_{observed}$ i.e. 50 mg/100 ml.

$NTU_{observed}$, $NTU_{expected}$ and $NTU_{plateau}$ are given in Table 3. As seen from the table, $NTU_{expected}$ and $NTU_{plateau}$ are in an overall close agreement suggesting that the formulas utilized in the dissolution studies did in fact melt and emulsify to the same extent as the formulas directly solublized prior to solidification. Any discrepancy could be due to imperfect capsule filling, media evaporation, and due to the method by which the samples were introduced to water in the two studies.

Lag phase of the turbidity–time profile reflects the time elapsed before the formula is released from the capsule into the dissolution medium. Fig. 10 correlates lag times with surfactant to co-surfactant ratios. Intercept of the regression line with the y-axes was at 4.98 min which is almost identical to the average break time for an empty HPMC capsule size 4 used in this study. Any deviation from this time should be correlated with the inherent properties of the fill material. Increase in cremophor EL to capmul MCM ratios from 0.5 to 3 delayed the onset of emulsion formation from 6.1 to 8.2 min, respectively. Increase in surfactant concentration delayed the onset of emulsification. At high cremophor EL concentration, progress of emulsification might be compromised by viscous liquid crystalline gel formed at the surfactant–water interface. It was reported that when a self-emulsified system is diluted by the aqueous phase various mesomorphic phases formed between the formula and the water (Iranloye et al., 1983). This was observed when the mesogenic properties of the formulation at different concentrations of each component were evaluated by studying the optical birefringence of the samples. In the absence of water, a droplet of surfactant (cremophor EL) and co-surfactant (capmul MCM-C8) placed in contact on a microscope slide revealed a boundary with no obvious signs of mixing and no optical birefringence as shown in Fig. 11a. When cremophor EL was mixed with water in the absence of co-surfac-

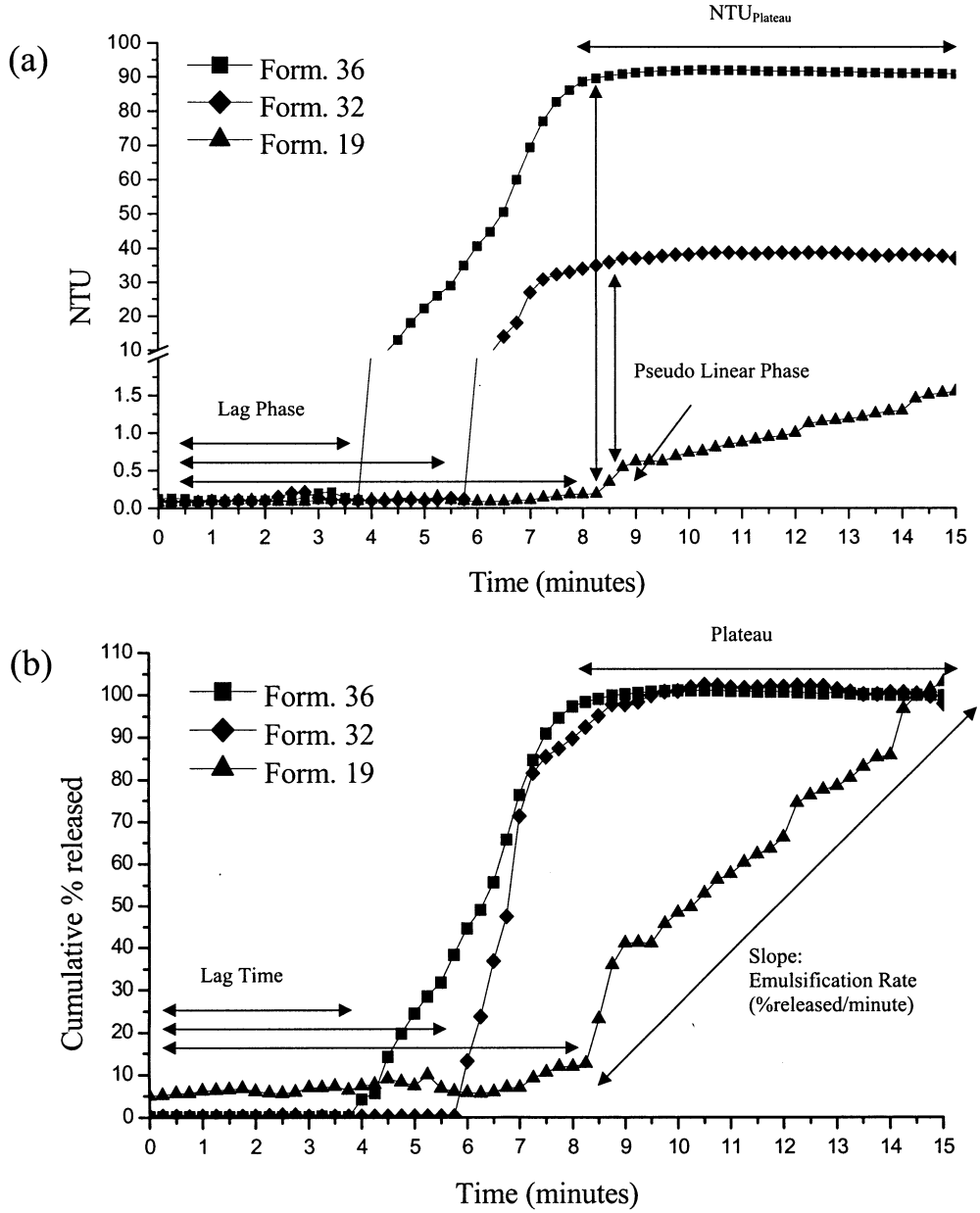

Fig. 9. (a) Turbidity–time profiles of three CoQ_{10} SNEDDS preparations. (b) Normalized turbidity–time profile showing the cumulative percent of CoQ_{10} released with time for the three CoQ_{10} SNEDDS preparations.

tant, the mixture showed birefringent texture of a gel (Fig. 11b). Addition of co-surfactant resulted in typical birefringent textures of non-gelled fluid lyotropic liquid crystalline phase as described below in a greater detail for a system with a fixed surfactant to co-surfactant weight ratio of 1:1.

Mixtures of surfactant:co-surfactant:water at weight proportions of 1:1:1 showed no signs of optical birefringence which were absent with an increase in water content up to a ratio of 1:1:2.5.

At a ratio of 1:1:3 the mixture revealed distinctive liquid crystalline textures when observed under the polarizing microscope as shown in Fig. 11c–e. Fig. 11c shows a birefringent texture of the 1:1:3 mixture with defect features similar to the so-called parabolic focal conic domains in lamellar (smectic) liquid crystals (Kleman, 1983). Fig. 11d shows another typical defect of the lamellar phase: the so-called oily streaks that represent the bundles of linear defects- dislocations, sometimes decorated with chains of focal conic domains (Boltenhagen et al., 1991). Fig. 11e shows an air bubble trapped in the mixture as seen under a regular setting with two crossed polarizers. The liquid crystal material is aligned near the surface of the bubble. Polarizing microscope fitted with crossed polarizers, with a quartz wedge inserted between the sample and the analyzer, showed a change in the interference colors around the air bubble that is consistent with an idea that the mixture is a lamellar type of the lyotropic liquid crystal (Kurik and Lavrentovich, 1983). Hence, a delay in the spontaneity of emulsion formation might be due to the time required for the transformation from one liquid crystalline structure to another during the first stages of the disruption process (Groves and de Galindez, 1976).

A cumulative percent of the formulation emulsified with time could be obtained by plotting cumulative turbidity given by $^{t}_{NTU} \times 100/NTU_{plateau}$ as a function of time, assuming that $NTU_{plateau}$ reflect 100% of the formula released from the capsules regardless of the actual amount of CoQ_{10} dissolved in the medium (Fig. 9b). $^{t}_{NTU}$ is the turbidity reading at any time t. Given re-arrangement allows directly correlating formulations with different turbidity–time profiles. As seen from Fig. 9b, plots of cumulative percent of the formulation released with time are identical to the original profiles correlating turbidity with time where curve characteristics mainly lag time, pseudo linear phase and plateau are preserved. Thus, slope of the pseudo linear phase for the line correlating cumulative percent emulsified with time could be regarded as the emulsification rate (E_{rate}) or emulsification efficacy. This value is very useful in comparing emulsification tendency of the self-emulsified preparation. Fig. 12 correlates emulsification rate with oil loading and surfactant to co-surfactant ratios. Maximum emulsification rate was obtained at a surfactant to co-surfactant ratio of 1 and oil loading of 42.6%. This might be due to an optimum HLB of the mixture. Bachynsky et al. (1997) showed that the HLB of the surfactant has a significant effect on the performance of the self-emulsifying system. However, optimum surfactant mixture should be obtained at an appropriate combination with the oily phase (Shah et al., 1994). At higher concentrations of the oily phase, proportion of the surfactant mix that facilitates water penetration decreases and the mixture becomes more lipophilic with increasing difficulty of emulsification (Halbaut et al., 1996). Thus, emulsion progress becomes less dependent on surfactant and co-surfactant concentrations.

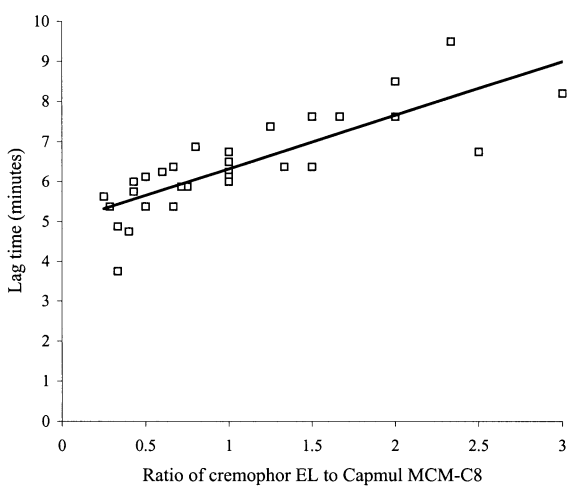

Fig. 10. Effect of surfactant (cremophor EL) to co-surfactant (capmul MCM-C8) ratios on lag time to self-emulsification.

4. Conclusion

The present investigation illustrated the potential use of eutectic mixtures with essential oils for the preparation of SNEDDS. Prepared SNEDDS improved the dissolution of CoQ_{10}. Recrystallization may add to the stability of the drug while providing attractive semisolid preparation that could be filled into hard HPMC capsules. Tur-

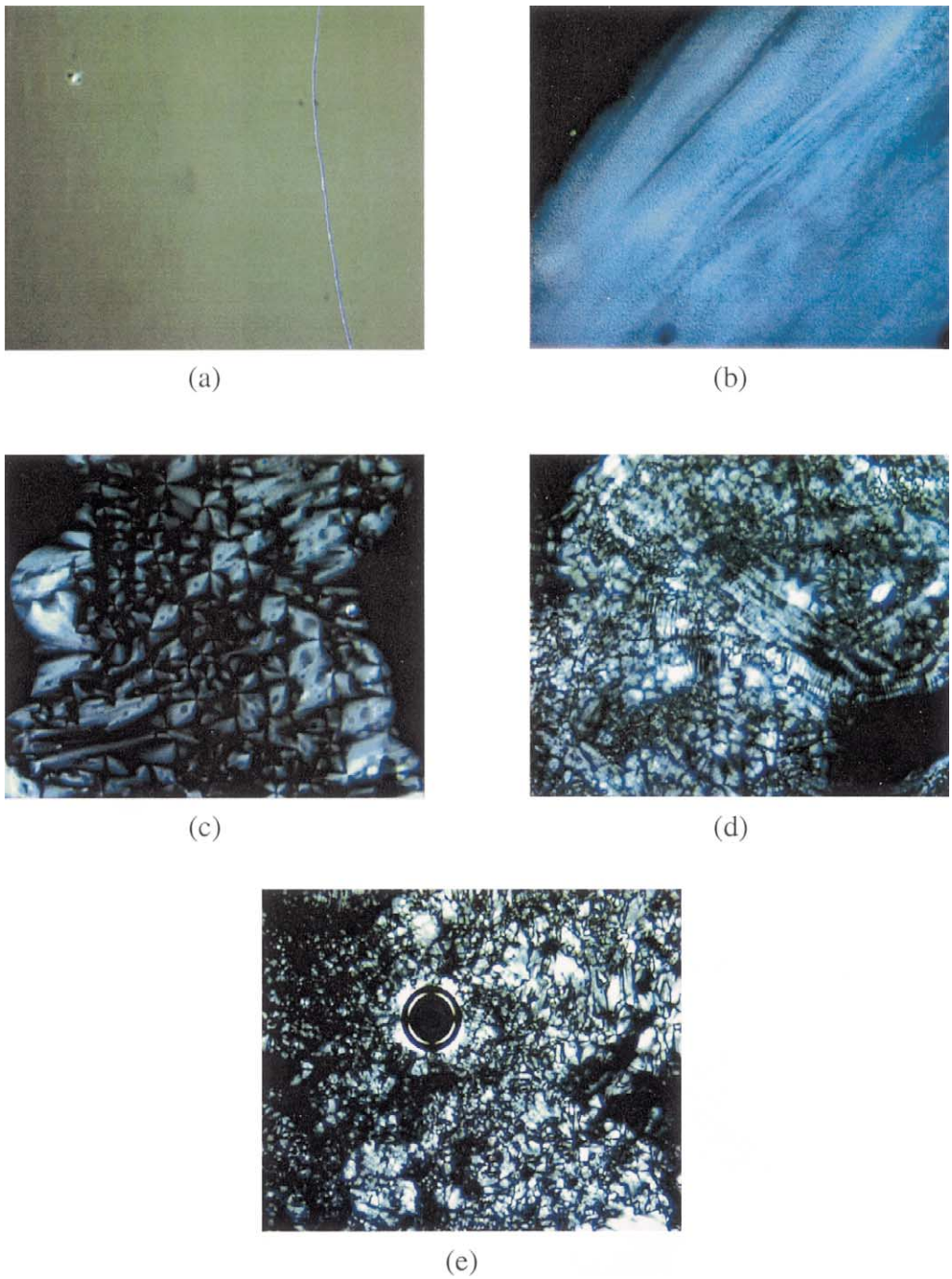

Fig. 11. (a) Optical microscope with no polarizers showing the texture of the surfactant, co-surfactant contact line; no birefringence. Polarizing microscope with crossed polarizers showing (b) birefringent texture of a gel formed in the mixture surfactant:water in weight proportion 1:3, (c) birefringent liquid crystalline texture of surfactant:co-surfactant:water mixture at a weight proportion of 1:1:3, (d) birefringent liquid crystalline texture with oily streaks at a mixture of 1:1:3, and (e) birefringent liquid crystalline texture of the mixture 1:1:3 with a trapped air.

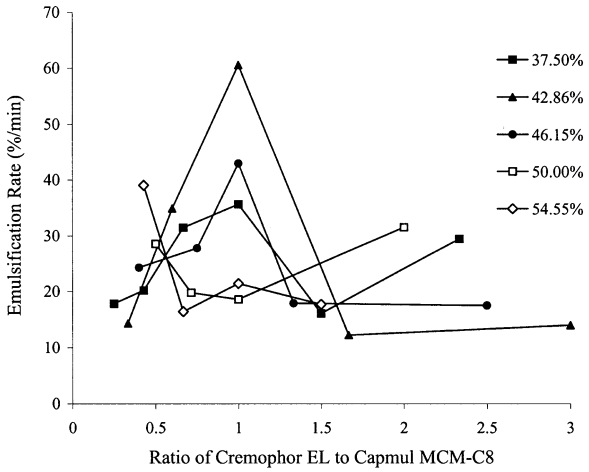

Fig. 12. Effect of surfactant (cremophor EL) to co-surfactant (capmul MCM-C8) ratios on the emulsification rate (E_{rate} is given as percent of the formula emulsified per minute).

bidimetry directly correlated emulsification rate, lag times and droplet size with formulation ingredients. This was used to distinguish between different self-emulsified preparations, which might be more important than simply identifying systems that are spontaneously emulsifying.

Acknowledgements

The authors wish to thank Dr Quentin Smith and Dean Nelson for their support in the establishment of a Center for Drug Delivery and Formulations at Texas Tech University School of Pharmacy. Appreciation is also extended to Dr Indra K. Reddy and Dr Ronda Akins for their invaluable help. The authors are also grateful to Dr Darren Williams at West Texas A&M University for his assistance with FT-IR analysis, and Dr Ted Zobeck and Dean Holder at the USDA-Agricultural Research Service for helping with particle size analysis.

References

Bachynsky, M.O., Shah, N.H., Patel, C.I., Malick, A.W., 1997. Factors affecting the efficiency of a self-emulsifying oral delivery system. Drug. Dev. Ind. Pharm. 23 (8), 809–816.

Benet, L.Z., Wacher, V.J., Benet, R.M., 1998. Use of essential oils to increase bioavailability of oral pharmaceutical compounds. United States Patent No. 5,716,928.

Boltenhagen, P., Lavrentovich, O., Kleman, M., 1991. Oily streaks and focal conic domains in L-α lyotropic liquid crystals. J. Phys. II France 1, 1233–1252.

Charman, S.A., Charman, W.N., Rogge, M.C., Wilson, T.D., Dutko, F.J., Pouton, C.W., 1992. Self-emulsifying drug delivery systems: formulation and biopharmaceutic evaluation of an investigational lipophilic compound. Pharm. Res. 9 (1), 87–93.

Chiwele, I., Jones, B.E., Podczeck, F., 2000. The shell dissolution of various empty hard capsules. Chem. Pharm. Bull. 48 (7), 951–956.

Chopra, R.K., Goldman, R., Sinatra, S.T., Bhagavan, H.N., 1998. Relative bioavailability of coenzyme Q10 formulations in human subjects. Int. J. Vitam. Nutr. Res. 68, 109–113.

Constantinides, P.P., Scalart, J.P., 1997. Formulation and physical characterization of water-in-oil microemulsions containing long- versus medium-chain glycerides. Int. J. Pharm. 158, 57–68.

Craig, D.Q.M., Lievens, H.S.R., Pitt, K.G., Storey, D.E., 1993. An investigation into the physico-chemical properties of self-emulsifying systems using low frequency dielectric spectroscopy, surface tension measurements and article size analysis. Int. J. Pharm. 96, 147–155.

Craig, D.Q.M., Barker, S.A., Banning, D., Booth, S.W., 1995. An investigation into the mechanisms of self-emulsification using particle size analysis and low frequency dielectric spectroscopy. Int. J. Pharm. 114, 103–110.

Gao, Z.G., Choi, H.G., Shin, H.J., Park, K.M., Lim, S.J., Hwang, K.J., Kim, C.K., 1998. Physicochemical characterization and evaluation of a microemulsion system for oral delivery of cyclosporin A. Int. J. Pharm. 161, 75–86.

Grossi, G., Bargossi, A.M., Fiorella, P.L., Piazzi, S., Battino, M., Bianchi, G.P., 1992. Improved high-performance liquid chromatographic method for the determination of coenzyme Q10 in plasma. J. Chromatogr. 593, 217–226.

Groves, M.J., Mustafa, R.M.A., 1974. Measurement of the 'spontaneity' of self-emulsifiable oils. J. Pharm. Pharmacol. 26, 671–681.

Groves, M.J., de Galindez, D.A., 1976. Rheological characterization of self-emulsifying oil/surfactant systems. Acta Pharm. Suecica. 13, 353–360.

Halbaut, L., Berbe, C., del Pozo, A., 1996. An investigation into physical and chemical properties of semi-solid self-emulsifying systems for hard gelatin capsules. Int. J. Pharm. 130, 203–212.

Hongve, D., Akesson, G., 1998. Comparison of nephelometric turbidity measurements using wavelengths 400–600 and 860 nm. Water Res. 32 (10), 3143–3145.

Iranloye, T.A., Pilpel, N., Groves, M.J., 1983. Some factors affecting the droplet size and charge of dilute oil-in-water emulsions prepared by self-emulsification. J. Disp. Sci. Technol. 4 (2), 109–121.

Jonker, G.H., 1952. Optical properties of colloidal solutions. In: Kruyt, H.R. (Ed.), Colloid Science. Elsevier, Amsterdam, pp. 90–114.

Kang, L., Jun, H.W., McCall, J.W., 2000. Physicochemical studies of lidocaine–menthol binary systems for enhanced membrane transport. Int. J. Pharm. 206, 35–42.

Kleman, M., 1983. Points, Lines and Walls in Liquid Crystals, Magnetic Systems, and Various Ordered Media. Wiley, Chichester, p. 322.

Kommuru, T.R., Ashraf, M., Khan, M.A., Reddy, I.K., 1999. Stability and bioequivalence studies of two marketed formulations of coenzyme Q10 in beagle dogs. Chem. Pharm. Bull. 47 (7), 1024–1028.

Kommuru, T.R., Gurley, B., Khan, M.A., Reddy, I.K., 2001. Self-emulsifying drug delivery systems (SEDDS) of coenzyme Q10: formulation development and bioavailability assessment. Int. J. Pharm. 212, 233–246.

Kurik, M.V., Lavrentovich, O.D., 1983. Monopole structures and shape of drops of smectic C. Zh. Eksp. Teor. Fiz. 85, 511–526 English translation: Sov. Phys. JETP, 58, 299–307.

Lawless, J., 1995. The Illustrated Encyclopedia of Essential Oils. Barnes & Noble, p. 120.

Lutka, A., Pawlaczyk, J., 1995. Inclusion complexation of coenzyme Q10 with cyclodextrins. Acta Polon. Pharm. 52 (5), 379–386.

Nazzal, S., Zaghloul, A.A., Reddy, I.K., Khan, M.A., 2001. Analysis of ubidecarenone (CoQ10) aqueous samples using reversed phase liquid chromatography. DiePharmazie 56 (5), 394–396.

Nazzal, S., Guven, N., Reddy, I.K., Khan, M.A., 2002. Preparation and characterization of coenzyme Q10—Eudragit® solid dispersion. Drug. Dev. Ind. Pharm. 28 (1), 49–57.

Nyqvist-Mayer, A.A., Brodin, A.F., Frank, S.G., 1986. Drug release studies on an oil–water emulsion based on a eutectic mixture of lidocaine and prilocarpine as the dispersed phase. J. Pharm. Sci. 75 (4), 365–373.

Pouton, C.W., 1985. Self-emulsifying drug delivery systems: assessment of the efficiency of emulsification. Int. J. Pharm. 27, 335–348.

Pouton, C.W., 2000. Lipid formulations for oral administration of drugs: non-emulsifying, self-emulsifying and 'self-microemulsifying' drug delivery systems. Eur. J. Pharm. Sci. Suppl. 2, S93–S98.

Reiss, H., 1975. Entropy-induced dispersion of bulk liquids. J. Colloid Interf. Sci. 53 (1), 61–70.

Sadar, M.J., 1998. Turbidity Science. HACH Technical Information Series. Booklet No. 11. HACH Company, Loveland, CO.

Shah, N.H., Carvajal, M.T., Patel, C.I., Infeld, M.H., Malick, A.W., 1994. Self-emulsifying drug delivery systems (SEDDS) with polyglycolyzed glycerides for improving in vitro dissolution and oral absorption of lipophilic drugs. Int. J. Pharm. 106, 15–23.

Takeuchi, H., Sasaki, H., Niwa, T., Hino, T., Kawashima, Y., Uesugi, K., Ozawa, H., 1992. Improvement of photostability of ubidecarenone in the formulation of novel powdered dosage form termed redispersible dry emulsion. Int. J. Pharm. 86, 25–33.

Yang, J., Her, J.W., 1999. Gas-assisted IR-ATR probe for detection of volatile compounds in aqueous solutions. Anal. Chem. 71, 1773–1779.